

Article

# Impact of the Initial State on BDS Real-Time Orbit Determination Filter Convergence

Yun Qing<sup>1</sup>, Yidong Lou<sup>1,\*</sup>, Yang Liu<sup>1,\*</sup>, Xiaolei Dai<sup>1</sup> and Yi Cai<sup>2</sup>

<sup>1</sup> GNSS Research Center, Wuhan University, 129 Luoyu Road, Wuhan 430079, China; yqing@whu.edu.cn (Y.Q.); xldai@whu.edu.cn (X.D.)

<sup>2</sup> CHINA R&D ACADEMY OF MACHINERY EQUIPMENT, Beijing 100089, China; caiy69@163.com

\* Correspondence: ydlou@whu.edu.cn (Y.L.); liudaweng@whu.edu.cn (Y.L.); Tel.: +86-027-6877-8595 (Y.L.); +86-027-6877-7305 (Y.L.)

Received: 24 November 2017; Accepted: 10 January 2018; Published: 15 January 2018

**Abstract:** High precision real-time orbit of navigation satellites are usually predicted based on batch estimation solutions, which is highly dependent on the accuracy of the dynamic model. However, for the BDS satellites, the accuracy and reliability of the predicted orbit usually decrease due to the inaccurate dynamic model or orbit maneuvers. To improve this situation, the sequential estimation Square Root Information Filtering (SRIF) was applied to determine the real-time BDS orbits. In the filter algorithm, usually a long period is required for the orbit to converge to the final accuracy, due to lack of accurate initial state. This paper focuses on the impact of the initial state with different a priori Standard Deviation (STD) on the BDS orbit convergence performance in both normal and abnormal periods. For the normal period, the Ultra-Rapid (UR) orbit products and the Broadcast Ephemerides (BRDC) used as initial orbits are discussed respectively. For the abnormal period, orbit maneuver is analyzed. Experimental results show that a proper a priori STD of initial state can significantly accelerate the orbit convergence, while a loose a priori STD takes more than 10 h to converge in the radial direction for the BDS GEO/IGSO/MEO satellites. When the UR orbit product is used as the initial orbit, the orbit of the IGSO/MEO satellites can converge to decimeter-level immediately. When the BRDC product is used, the accuracy of meter-level can be obtained for the IGSO/MEO immediately, and converge to decimeter-level in about 6 h. For the period after the orbit maneuver, the real-time orbit accuracy can reach meter-level in about 6 h after the first group of broadcast ephemerides is received.

**Keywords:** Square Root Information Filter (SRIF); orbit maneuver; a priori; initial state; Standard Deviation; Rapid Convergence

## 1. Introduction

The Global Navigation Satellite System (GNSS) aims at serving high-precision real-time positioning, navigation and timing applications. The BeiDou Satellite Navigation System (BDS) developed by China is currently an operational constellation with five satellites in Geostationary Earth Orbit (GEO), six in Inclined Geosynchronous Satellite Orbit (IGSO) and four in Medium Earth Orbit (MEO). However, the MEO satellite C13 was deactivated due to unknown reasons. On 11 October 2016, the Pseudo Random Noise code (PRN) of BDS IGSO 6 switches from C15 to C13. The system will be evolving towards its global navigation capability with a full constellation consisting of 5 GEO, 3 IGSO and 27 MEO satellites by 2020 (<http://www.beidou.gov.cn/>) [1].

High-precision and reliable orbit product is a prerequisite for satellite navigation and positioning services. The orbit products can be determined by two means, one is the batch estimation Least-Squares (LSQ) processing, and the other is the sequential estimation filtering processing [2]. For the moment, the real-time orbit of navigation satellites is usually predicted based on the batch processing, which

is highly dependent on the accuracy of the dynamic model. However, for the current BDS-2 regional navigation system, there are many factors that reduce the accuracy and reliability of the predicted orbit [3–15], including the regional distribution of stations [3–7,9], orbit maneuvers, the inaccurate dynamic force model [12–14] and the switching of different attitude modes. In detail, the orbit maneuvers occur frequently for the GEO satellites and occasionally for the IGSO and MEO satellites [16]. During the orbit maneuver, the force models acting on the satellite changes irregularly, thus, the original dynamic model is no longer accurate to represent the real orbit of the satellite. In addition, for the GEO satellites, due to the geostationary orbit characteristics and the orbit-normal attitude mode, the existing Solar Radiation Pressure (SRP) model is inadequate to describe their SRP force accurately leading to the orbit accuracy decreases [12,13]. Moreover, for the IGSO/MEO satellites, it is not possible to fit two orbit states with one set of SRP parameters due to the change of force model during the attitude scheme switching period between the yaw-steering and the orbit-normal mode, resulting in decreased orbit accuracy using the traditional LSQ method [17–19]. To overcome these problems and provide a stable real-time orbits and clocks products, one solution is adjusting both orbits and clocks in real time using the sequential estimation filter.

The Real-Time GPS Inferred Positioning System (GIPSY) (RTG) software developed by the Jet Propulsion Laboratory (JPL) based on Upper and Diagonal (UD) factorization filter can provide real-time estimates of the GPS orbits and 1 Hz GPS clocks [20]. After years of development and updates, the new Operational Control System (OCX) orbit determination software, called RTGX, is derived from JPL's RTG and GIPSY software. Different from the RTG's filter algorithm, RTGX reverts to GIPSY's SRIF formulation which can provide the real-time satellite orbits and clocks of GPS, GLONASS, BDS and Galileo ([21]; <http://www.gdgps.net/>). In mid of 2011, Trimble introduced the CenterPoint RTX real-time positioning service providing positions with centimeter-level accuracy, in which the satellite orbits are estimated using a combination of a UD-factorized Kalman filter. The RTX has GPS, GLONASS and QZSS in full operation in 2012 and has completed the trial operation of Galileo and BDS in 2013 [22,23]. The France Centre National d'Etudes Spatiales (CNES) employed a Kalman filter to determine the real-time satellite orbits and clocks. The results showed an accuracy of 5, 10, 18, 18 and 36 cm for GPS, GLONASS, Galileo, BeiDou MEO and BeiDou IGSO [24]. The ESA Auto-BAHN software [25,26] under development at Newcastle University introduced the Extended Kalman Filter approach to obtain GPS satellite orbits and clocks, and the results showed that the mean 3D RMS of the orbit accuracy reached 13.6 cm [27].

In this contribution, the adaptive SRIF is employed to determine the BDS real-time orbits. The filtering algorithms always have a convergence process, and need re-convergence when orbit anomalies occur, such as orbit maneuvers. Therefore, how to accelerate initial convergence and re-convergence especially when orbit maneuver occurs are of great importance. Generally, the accuracy of the initial orbits (satellite Position and Velocity-PV, Solar Radiation Parameters-SRP) and the a priori Standard Deviation (STD) have the greatest influence on the convergence time, thus are mainly discussed in this paper. Normally, the initial orbits can be obtained from IGS Ultra-Rapid (UR) products or the broadcasting ephemerides (BRDC) products in normal periods. When orbit maneuver occurs in abnormal periods, the original orbit parameters are no longer applicable. Thus, for simplicity, the filtering process of the maneuver satellite is suspended in this paper until the first group broadcast ephemeris of this satellite can be received. Therefore, the PV parameters can be initialized with the broadcast ephemerides and the SRP parameters can be initialized with the estimated value of the filter before the maneuver with appropriate constraints. This paper mainly focuses on the impact of the initial state (PV and SRP) with different a priori STD on the filter convergence performance of BDS orbit determination in both normal and abnormal periods.

The orbit products users can obtain are the predicted orbit based on the determined part. Usually, the orbit filter has a measurement update interval of several seconds or minutes, and the orbit products are generated correspondingly. Due to the short time delay, the orbit accuracy loss of the predicted orbit can be neglected when there is no satellite maneuver. Therefore, the convergence performance of

the determined orbit can almost represent that of the predicted orbit. In this study, the determined orbit of the filter is used to assess the convergence performance.

The paper is organized as follows. Section 2 briefly describes the orbit determination strategy for data processing and data sets for normal and abnormal periods. In Section 3, the filter model adopted in this paper is introduced, and then the strategy to obtain the optimal a priori STD magnitude of the PV and SRP parameters in normal periods is presented. The corresponding experimental results and the impact of initial orbits with different a priori STD on orbit convergence are analyzed in Section 4. Finally, the conclusions are summarized in Section 5.

## 2. Materials and Methods

### 2.1. Orbit Determination Strategy

The Positioning and Navigation Data Analyst (PANDA) software [28] developed by the GNSS Research Centre of Wuhan University was adapted for BDS data processing in this study. The orbit-normal attitude mode is adopted for the BDS GEO satellites, and the BDS IGSO and MEO satellites maintain the yaw-steering attitude most of the time and enter into the orbit-normal attitude mode when the elevation of the sun w.r.t. the orbital plane is below a threshold of about 4 degree [29]. All the BDS IGSO and MEO satellites are in the yaw-steering attitude mode in our analyzed period. For BDS satellites, the phase center offsets (PCO) values estimated by ESA [30] are adopted and no phase center variations (PCV) are applied. The specific orbit determination strategy for the filter is shown in Table 1.

**Table 1.** Orbit determination strategy.

Item	Contents
Solar Radiation Pressure	ECOM 5-parameter [31–33]
Geopotential	EGM 2008 model (12 × 12)
M-body gravity	Sun, Moon and planets
Tidal forces	Solid Earth, pole, ocean tide IERS Conventions 2010 [34]
Relativistic effects	IERS Conventions 2010 [34]
Numerical integration	Runge-Kutta for single step integration, Adams for multistep integration
Reference frame	IGS08
Basic Observables	un-differenced BDS B1/B2 ionosphere-free combination of code and phase
Sampling rate	300 s
Cutoff elevation	7°
Weighting	Elevation-dependent, 1 for $E > 30^\circ$ , otherwise $2 \times \sin(E)$
Satellite antenna phase center	Only PCO correction for all BeiDou satellites [30]
Receiver antenna	Use GPS values [35]
Earth rotation parameters (ERP)	IERS 08 C04 [36]

### 2.2. Filter Model

The Kalman filtering algorithm is sensitive to computer roundoff and its numeric accuracy sometimes degrades to the point where the results cease to be meaningful. To overcome its potential numeric inaccuracy and instability, the Square Root Information Filter (SRIF) which is an evolutionary version of the Kalman filter has been derived [37]. The SRIF algorithm has the following characteristics,

i.e., it has inherently lower storage requirements, better stability and numeric accuracy than the Kalman filter.

The function model of the SRIF can be described by a state equation with random initial conditions, dynamic noise, and discrete observation equations. At the epoch  $t_0, t_1, \dots, t_k, \dots$ , the initial state conditions, the state equation and the observation equation can be expressed as:

$$\begin{cases} X_{k+1} = \Phi_{k+1,k}X_k + \Omega_{k+1} \\ L_{k+1} = B_{k+1,k}X_{k+1} + \Delta_{k+1} \end{cases}$$

where  $X_k, X_{k+1}$  are the state parameters of epochs  $t_k, t_{k+1}$  respectively, and  $L_{k+1}$  is the observation vector of  $t_{k+1}$ .  $\Phi_{k+1,k}$  is the state transition matrix,  $\Omega_{k+1}$  is the process noise.  $B_{k+1,k}$  is the coefficient design matrix of observations,  $\Delta_{k+1}$  is the observation noise. The a priori STD of phase observations is set to 1 mm. Taking into account the 300 s sampling interval and in accordance with the research of Laurichesse et al. [24], the process noise of the stochastic orbit parameters (SRP and PV) are set to  $10^{-13}$ ,  $10^{-13}$  m and  $10^{-13}$  m/s respectively, which are proved to be valid in this paper.

In addition, the a priori information of the initial state  $X_0$  should be considered. Specifically, the a priori expectation of  $X_0$  can be taken as a virtual observation along with the a priori STD  $\sigma(X_0)$  as the corresponding noise. In this paper, we mainly study the influence of the initial orbits (SRP and PV) with different a priori STD  $\sigma(X_0)$  on the convergence performance of BDS orbit determination. The a priori STD is closely related to the accuracy of the initial orbits. As mentioned before, the initial orbits obtained from the UR and BRDC products are discussed respectively in normal period. When the orbit maneuver occurs, the initial value of the PV can be obtained from the broadcast ephemerides and the SRP from the estimated value of the filter before the maneuver along with appropriate constraints. In the above two cases, the initial accuracy of the SRP and PV parameters are different. Therefore, the a priori STD  $\sigma(X_0)$  should be adjusted accordingly. Generally, the a priori STD should be a large value when the initial accuracy is low and be a small value when the accuracy is high. The strategies for the selection of the a priori STD are presented in the next section.

### 2.3. Data Collection

In the experiment, all the IGS Multi-GNSS Experiment (MGEX) stations tracking BDS were used. In 2012, the MGEX has been set-up by the IGS to track, collate and analyze all available GNSS signals [15]. Up to March 2017, about 150 MGEX stations were available, and about 100 stations can track BDS (<http://mgex.igs.org/>). Figure 1 shows the BDS tracking stations used in this paper.

Two sets of MGEX data were collected in our experiment for the BDS normal and abnormal period respectively. For the normal period, the data span 20 days from DOY 138, 2016 to 157, 2016 is used. During the experiment period, there are 5 GEO satellites (C01~C05), 6 IGSO satellites (C06~C10, C15) and 3 MEO satellites (C11, C12, C14) available. In order to analyze the convergence performance, consecutive 36-h arc using the SRIF solution are processed with the start epoch shifted by 1 day each. Each process covers 36-h arc to ensure that the orbit has converged. Then the average convergence performance is taken for analysis.

For the abnormal period, orbit maneuver is taken as an example. The GEO satellite C05 and the IGSO satellite C08 were selected. The maneuver time of C05 is from 23:54 on DOY 186, 2015 to 1:14 on DOY 187, 2015, and the first group broadcast ephemeris was received at 06:00 on DOY 187, 2015. The maneuver time of C08 is from 13:35 to 14:50 on DOY 009, 2015, and the first group broadcast ephemeris was received at 20:00 on the same day. The filter is processed using only BDS system to test the convergence capability.

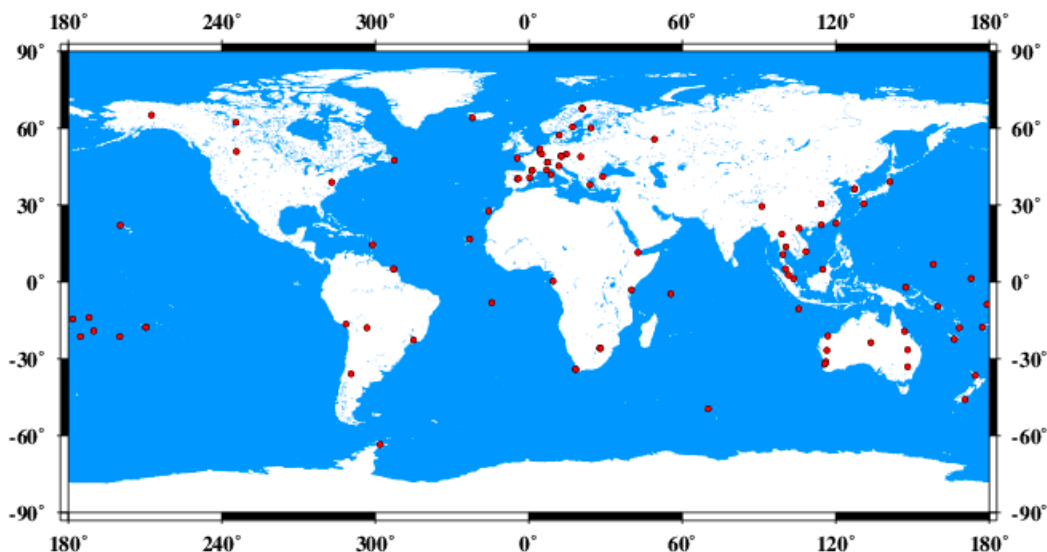


**Figure 1.** Distribution of MGEX stations used for BDS orbit determination. This figure is drawn using GMT software [38].

2.4. Experimental Design

In this section, the strategy to obtain the a priori STD in normal period is discussed. In this paper, the UR and BRDC products are used as the initial orbits (Figure 2). To avoid systematic bias of other analysis centers, especially for the GEO satellites, the UR product is produced by the PANDA software using batch estimation. The UR product consists of the observed part and the prediction part. To ensure the orbit accuracy of the UR product, GPS and BDS joint orbit determination is carried out in the observed part using LSQ solution with 3-day arc length. In this case, the a posteriori STD  $\sigma(X)$  of the observed part can be used as the base value of the a priori STD in the SRIF filter solution. Generally, the observed orbits always have a latency of 3~9 h when they are accessible, which will result in orbital accuracy loss. Therefore, the a priori STD of the filter should be loosened to a certain degree. Similarly, for the BRDC, as the orbit accuracy is lower than the UR product, the a priori STD value of the filter still uses the a posteriori STD of the LSQ solution as base value but should loosen more.

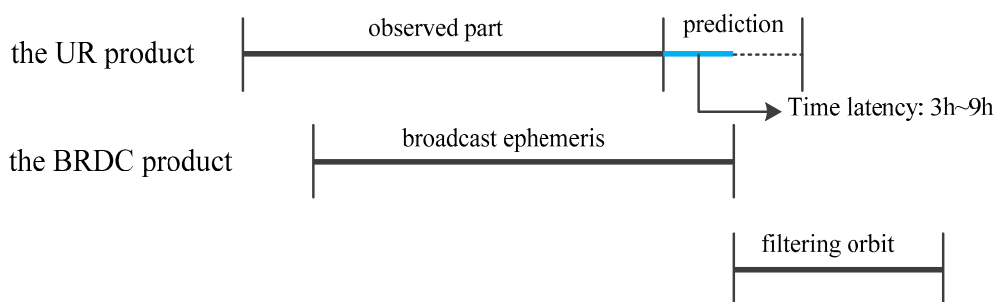


**Figure 2.** The initial orbit of SRIF filter orbit solution from the Ultra-Rapid products and the Broadcast Ephemerides.

From the above analysis, consecutive 3-day arc LSQ solution is processed using the first set of MGEX data in Section 2.3. Then, the a posteriori STD  $\sigma(X)$  of the orbit parameters (PV and SRP) can be obtained. Since the a posteriori STD of each orbit parameter for the same satellite type is in the same order of magnitude, the average a posteriori STD for different satellite types (GEO/IGSO/MEO) is given in Table 2. It can be observed that the a posteriori STD varies with different satellite type. Specifically, the GEO satellite positions have the accuracy of decimeter-level and the IGSO and MEO

satellites show similar accuracy of centimeter-level, which are about one order of magnitude smaller than that of the GEO satellites. For the SRP parameters, the a posteriori STD for the GEO/IGSO/MEO satellites is similar in the order of magnitude.

**Table 2.** Average a posteriori STD of PV and SRP parameters of LSQ solutions.

Satellite Type	$\sigma_0(X_{pv})$ (Unit: m; m/s)						$\sigma_0(X_{srp})$ (Unit: m/s <sup>2</sup> )				
	PX	PY	PZ	VX	VY	VZ	D0	Y0	B0	BC1	BS1
GEO	$3.4 \times 10^{-1}$	$5.4 \times 10^{-1}$	$1.9 \times 10^{-2}$	$4.0 \times 10^{-5}$	$2.5 \times 10^{-5}$	$1.0 \times 10^{-6}$	$7.0 \times 10^{-12}$	$2.0 \times 10^{-12}$	$2.6 \times 10^{-11}$	$1.9 \times 10^{-10}$	$8.9 \times 10^{-11}$
IGSO	$8.0 \times 10^{-3}$	$1.2 \times 10^{-2}$	$9.5 \times 10^{-3}$	$8.6 \times 10^{-7}$	$4.4 \times 10^{-7}$	$5.9 \times 10^{-7}$	$6.7 \times 10^{-12}$	$1.3 \times 10^{-12}$	$1.5 \times 10^{-11}$	$4.7 \times 10^{-11}$	$2.5 \times 10^{-11}$
MEO	$1.0 \times 10^{-2}$	$1.0 \times 10^{-2}$	$1.1 \times 10^{-2}$	$1.3 \times 10^{-6}$	$1.4 \times 10^{-6}$	$1.2 \times 10^{-6}$	$3.6 \times 10^{-11}$	$1.5 \times 10^{-12}$	$3.4 \times 10^{-11}$	$2.1 \times 10^{-10}$	$5.7 \times 10^{-11}$

The a posteriori formal errors listed in Table 2 serve as the base value of the a priori formal errors for the initial orbits of the filter. After obtaining the base value of the a priori STD for the initial orbits of the filter, the experimental scheme using the UR and BRDC as the initial orbits can be designed according to the accuracy of these two orbit products. From the previous analysis, the UR product has a latency of about 3 h~9 h, and the orbit accuracy decreases with the increasing time delay. In detail, Table 3 gives the orbit accuracy of the UR products with 3-h and 9-h latency, as well as the BRDC product. The multi-GNSS orbit product (GBM) of GeoForschungsZentrum Potsdam (GFZ) is used to evaluate the orbit of the BeiDou IGSO and MEO satellites. Besides, due to the large systematic bias for the BeiDou GEO satellites among different analysis centers, the orbit product estimated using LSQ solution by PANDA (WHU) is used to evaluate the BeiDou GEO satellite orbits. For the UR products, the orbit accuracy varies little for different latency in the cross-track and radial directions, while the accuracy loss mainly occurs in the along-track direction. For the BRDC, the orbit accuracy is at the meter-level and also worst in the along-track direction.

**Table 3.** Orbit accuracy of Ultra-Rapid products and Broadcast Ephemerides.

Initial Orbit Type	Time Latency	GEO (mm)			IGSO (mm)			MEO (mm)		
		A	C	R	A	C	R	A	C	R
Ultra-Rapid products	3 h	357	201	117	217	132	88	94	56	32
	9 h	474	198	112	259	130	90	138	58	33
Broadcast Ephemerides	/	6180	518	244	1197	1041	321	1290	631	406

Based on the accuracy of the UR and BRDC products, different a priori STD of initial state (PV and SRP) are analyzed for orbit convergence as shown in Table 4. To isolate the impact of initial PV and SRP parameters on orbit convergence, these two kinds of parameters with different a priori STD will be discussed separately in Section 4. Then, the final convergence performance is analyzed based on the optimal a priori STD magnitude. To access the impact of SRP parameters on the convergence, the a priori STD of PV parameters are set fixed to the same value as that of the reference orbit (Table 5 in Section 3.1). Similarly, to access the impact of PV parameters on the convergence, the a priori STD and initial value of SRP parameters are also set fixed to the same value as that of the reference orbit. Specifically, when the UR product is used as the initial orbit, the initial value of PV is from the prediction arc and that of SRP is the estimated value of the observed arc. When the BRDC product is used as the initial orbit, the initial value of PV is from the broadcasting ephemerides and that of SRP is obtained by fitting the broadcasted orbits with 3-day arc before the start epoch of each filtering process.

The above discussion focuses on experimental design under satellite normal period, which will be discussed in detail in Sections 3.2 and 3.3. Then, orbit maneuver will be analyzed as an example of orbit anomalies in Section 3.4.

**Table 4.** Experiment scheme of the convergence analysis in normal period.

Initial Orbit Type	Parameter	$\Delta t$ (h)	The A Priori STD of the Initial Orbit		
Ultra-Rapid Products	SRP	3 h	$\sigma_0(X_{srp})$	$10 \times \sigma_0(X_{srp})$	$100 \times \sigma_0(X_{srp})$
		9 h	$\sigma_0(X_{srp})$	$10 \times \sigma_0(X_{srp})$	$100 \times \sigma_0(X_{srp})$
	PV	3 h	$\sigma_0(X_{pv})$	$10 \times \sigma_0(X_{pv})$	$100 \times \sigma_0(X_{pv})$
		9 h	$\sigma_0(X_{pv})$	$10 \times \sigma_0(X_{pv})$	$100 \times \sigma_0(X_{pv})$
Broadcast Ephemerides	SRP	/	$10 \times \sigma_0(X_{srp})$	$100 \times \sigma_0(X_{srp})$	$1000 \times \sigma_0(X_{srp})$
	PV	/	$10 \times \sigma_0(X_{pv})$	$100 \times \sigma_0(X_{pv})$	$1000 \times \sigma_0(X_{pv})$

### 3. Convergence Performance Analysis and Results

In this section, the post processed orbit products estimated by LSQ method are used to evaluate the accuracy of the orbit estimated by SRIF. As mentioned before, the orbit product calculated by PANDA software adopted in this paper (WHU) is used to evaluate the GEO satellite orbits as systematic bias exists in the products of different analysis center. The orbit product (GBM) of GFZ is used to evaluate the orbit of the IGSO and MEO satellites.

#### 3.1. Orbit Convergence with Loose A Priori Constraints

To make a distinct comparison among the filter orbits with different a priori STD and emphasize the impact of initial SRP and PV on convergence of the filter, the convergence of the orbit with loose a priori constraints is given in this section. Under this condition, the PV parameters are initialized with the broadcast ephemerides and the SRP parameters are initialized to zero. Loose a priori STD of the initial state is adopted in this section as listed in Table 5. In the following analysis, the symbol ‘REF’ refers to the orbit using the a priori STD in Table 5. Using the first set of MGEX data in Section 2.3, the convergence time series of the average orbit accuracy are plotted in Figure 3.

**Table 5.** A priori STD of initial state.

Parameter	A Priori STD
Satellite Position	1 km
Satellite Velocity	1 m/s
Solar Radiation Pressure	$10^{-4}$ m/s <sup>2</sup>

The results show that for the GEO satellites, the accuracy of the along-track is worse than the cross-track and radial direction. Meanwhile, for the IGSO and MEO satellites, it takes the longest time to converge to the final accuracy in the radial direction than in the cross and along directions. The convergence time of orbit filter is related to the orbit type of navigation satellites. The convergence time of the MEO satellites is the shortest while that of the GEO satellites is the longest, because the dynamic model and observation geometry of MEO satellites is better than that of the GEO and IGSO satellites. The geometric observation structure for the GEO satellites keeps almost unchanged because of the geostationary characteristics, resulting in longer convergence time.

From the above analysis, it can be noticed that satellites of the same type have similar convergence performance. Accordingly, convergence performance will be analyzed in terms of different satellite types instead of each satellite separately in the following discussion. The empirical orbit convergence criteria adopted in our study is 10 consecutive hours of orbit in the defined range of accuracy as follows: for the IGSO and MEO satellites, the accuracy is less than 60 cm in the along-track, cross-track and radial direction; for the GEO satellites, the accuracy is less than 100 cm in the along-track and 80 cm in the cross-track and radial direction. In order to reflect the convergence time numerically, the convergence time of each scheme will be calculated.

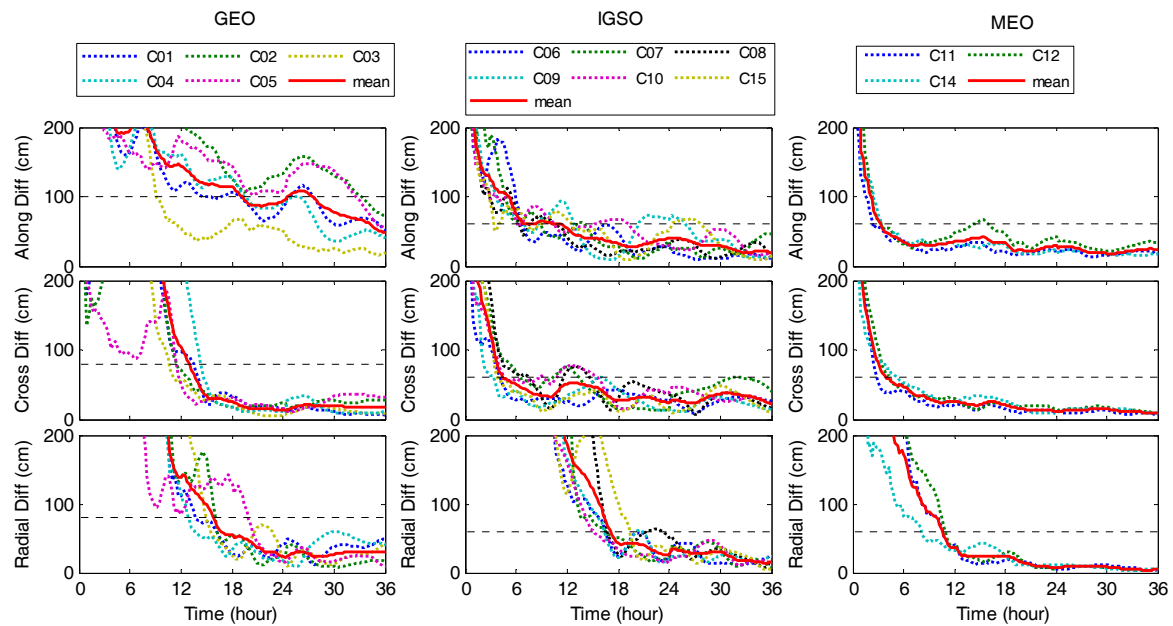


**Figure 3.** Time series of the average accuracy of the reference orbit. The red line represents the average time series of the satellites of the same type. The horizontal black dotted line represents the convergence criteria for each direction.

### 3.2. Orbit Convergence with Initial Orbit from UR Product

In this section, the impact of using the UR product as the initial orbit on the convergence performance will be discussed. Based on the scheme specified in Table 4, the convergence experiments are carried out using the first set of data described in Section 2.3. As the UR product has latency, the average convergence time of each satellite type using different a priori STD in both 3-h latency and 9-h latency are listed in Table 6. At the same time, the convergence time of the REF orbit (Figure 3) is calculated for comparison. To show the convergence process, Figures 4 and 5 depict the time series of the average filtering orbit accuracy in 3-h latency. Figure 4 shows the impact of different a priori STD of SRP parameters on orbit accuracy and Figure 5 shows the impact of different a priori STD of PV parameters on orbit accuracy. Furthermore, the time series of the average orbit accuracy with loose a priori constraints (REF) is also plotted in red line in Figures 4 and 5 for comparison.

From Table 6, it can be observed that there are obvious improvements of the convergence time when using the UR product as the initial orbit with proper a priori STD. Specifically, for the GEO satellites, the SRP parameters mainly affect the convergence time of the cross-track and radial directions, while the PV parameters more affects the along-track and cross-track directions. For the IGSO and MEO satellites, the SRP parameters mainly affect the convergence of the radial directions and the PV parameters primarily affect that of the along-track and cross-track directions. It implies that the SRP parameter has a strong correlation with the radial direction for the GEO, IGSO and MEO satellites. Besides, the convergence time of SRP parameters with two time delay (3 h and 9 h) has the similar values, which is because the effective effect of a set of high precision SRP parameters can maintain even for several days, so the impact on the orbit accuracy is not significant in a short time delay. Meanwhile, the orbit accuracy is close in 3-h and 9-h latency (see Table 3). Therefore, the convergence time of PV parameters with the same a priori STD does not change much in these two latencies.

From the time series of filtering orbit accuracy in Figures 4 and 5, it can be noticed that the orbit accuracy at the later stage of the filtering is deteriorated if the constraints of the a priori STD are too tight, even if it shows good accuracy at the beginning of the filter (see the blue line in Figures 4 and 5). This phenomenon is most obvious for the GEO satellites, which is due to the less accurate dynamic

model and the worst orbit accuracy among the three types of satellites. In this way, the a priori STD of the GEO satellites should be loosened.

According to the above analysis and the experimental results shown in Table 6, Figures 4 and 5, the optimal a priori STD magnitude of SRP and PV parameters are summarized in Table 7 for 3-h latency UR products. The time series of the average orbit accuracy using the optimal a priori STD magnitude is plotted in Figure 6. Meanwhile, the REF orbit accuracy is also given in dotted line for comparison. The results show that the orbit accuracy can reach decimeter-level immediately after the filter startup, which has a great improvement w.r.t. the REF orbit. Moreover, due to the use of high-precision SRP parameters as initial values along with proper constraints, the radial directions can converge rapidly instead of requiring more than 10 h to converge. Through the analysis of orbit convergence performance by using the UR product as the initial orbit, it can be found that the orbit accuracy can reach to the accuracy of decimeter-level in the first few minutes with proper a priori constraints.

**Table 6.** The average convergence time of the filter orbit using different a priori STD when the UR product is used as the initial orbit. Both 3-h and 9-h latency are calculated. Unit [hour]. For the GEO satellites, the convergence criteria adopted in our study are 100 cm in the along-track, and 80 cm in the cross-track and radial direction. For the IGSO and MEO satellites, the criteria are 60 cm in three directions.

Para.	Delay	$\sigma(\tilde{\epsilon}_0)$	GEO			IGSO			MEO		
			A	C	R	A	C	R	A	C	R
SRP	3 h	$\sigma_0(X_{srp})$	19.16	3.31	5.05	8.18	6.06	5.69	4.91	1.97	2.57
		$10 \times \sigma_0(X_{srp})$	19.52	3.44	5.09	7.75	5.51	5.72	5.15	1.96	2.57
		$100 \times \sigma_0(X_{srp})$	20.14	4.86	5.96	8.83	6.68	6.98	5.86	2.87	4.83
	9 h	$\sigma_0(X_{srp})$	19.05	3.34	5.01	7.85	6.14	5.65	4.9	1.97	2.58
		$10 \times \sigma_0(X_{srp})$	19.24	3.47	5.00	7.91	5.63	5.68	5.15	1.97	2.58
		$100 \times \sigma_0(X_{srp})$	19.67	4.79	5.88	8.92	6.64	6.98	5.86	2.93	5.16
PV	3 h	$\sigma_0(X_{pv})$	2.48	0.93	22.13	1.21	2.3	10.74	2.84	1.26	5.50
		$10 \times \sigma_0(X_{pv})$	15.44	1.40	17.70	1.80	2.39	12.36	1.92	0.64	6.33
		$100 \times \sigma_0(X_{pv})$	20.15	8.65	15.62	9.10	7.35	17.60	5.54	3.90	10.05
	9 h	$\sigma_0(X_{pv})$	6.58	0.66	21.81	1.03	3.27	10.62	3.20	0.79	6.02
		$10 \times \sigma_0(X_{pv})$	15.81	1.43	18.10	1.42	2.76	12.56	2.58	0.42	6.74
		$100 \times \sigma_0(X_{pv})$	19.16	8.90	15.45	9.88	8.04	18.18	5.88	4.13	9.98
REF			20.74	12.33	16.12	14.59	10.08	19.52	7.39	5.93	10.82

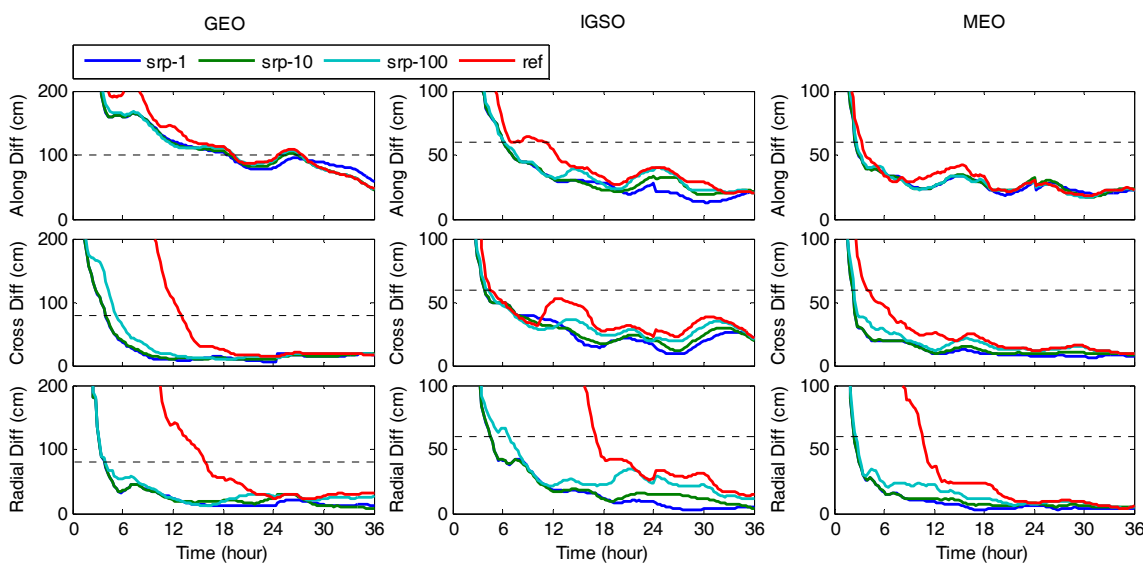


**Figure 4.** Time series of the average orbit accuracy using different a priori STD of SRP parameters. The UR product is used as the initial orbit and the latency time is 3 h. The horizontal black dotted line represents the convergence criteria for each direction.

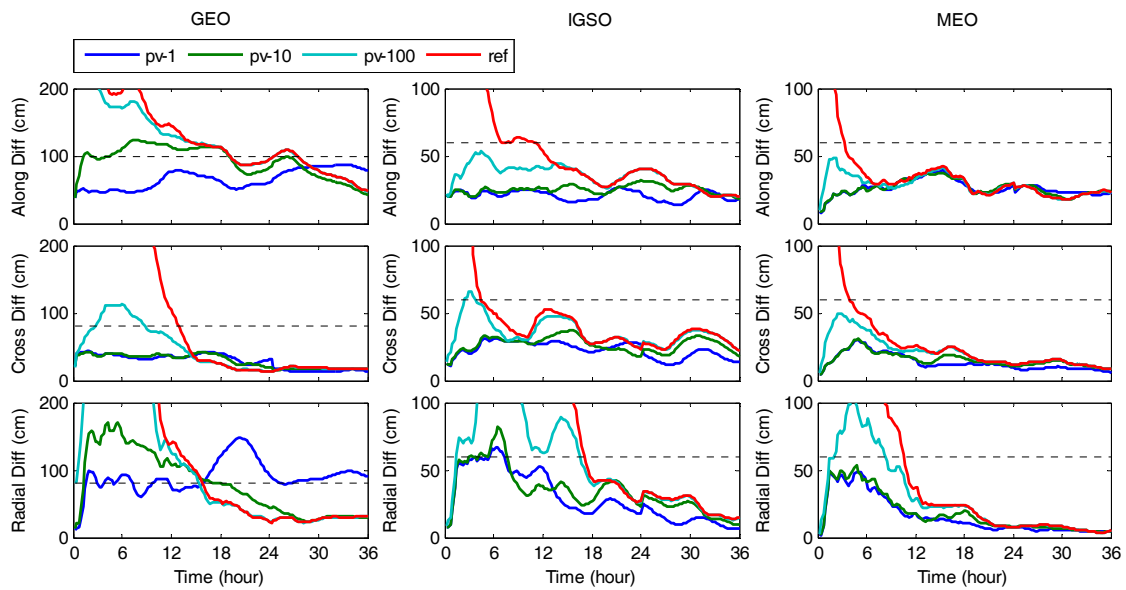


**Figure 5.** Time series of the average orbit accuracy using different a priori STD of PV parameters. The UR product is used as the initial orbit and the latency time is 3 h. The horizontal black dotted line represents the convergence criteria for each direction.

**Table 7.** Optimal a prior STD magnitude of SRP and PV parameters when the UR product is used as the initial orbit.

Parameter	GEO	IGSO	MEO
SRP	$10 \times \sigma_0(X_{srp})$	$1 \times \sigma_0(X_{srp})$	$1 \times \sigma_0(X_{srp})$
PV	$10 \times \sigma_0(X_{pv})$	$10 \times \sigma_0(X_{pv})$	$10 \times \sigma_0(X_{pv})$

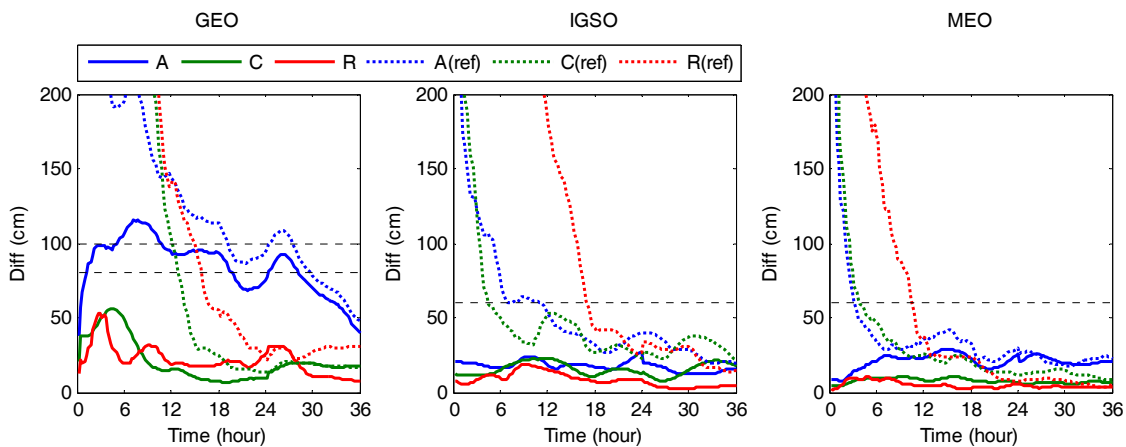


**Figure 6.** Time series of the average the accuracy of the filter orbits with the optimal a priori STD magnitude. The UR product is used as the initial orbit and the latency time is 3 h. The dotted line represents the accuracy of the REF orbits described in Section 3.1. The horizontal black dotted line represents the convergence criteria for each direction.

### 3.3. Orbit Convergence with Initial Orbit from BRDC Product

In the following analysis, the impact of using the BRDC as the initial orbit on the convergence performance is discussed based on the scheme in Table 4. The first set of MGEX data in Section 2.3 is adopted. Similar to the analysis of influence of the UR product on the filter convergence, Table 8 presents the average convergence time of each satellite type using different a priori STD (see Table 2).

Meanwhile, Figures 7 and 8 plot the time series of the average filtering orbit accuracy using different a priori STD. Similarly, the time series of the average orbit accuracy with loose a priori constraints (REF) is also given in red line as a comparison.

The results show that the influence of different a priori STD of SRP and PV parameters in the along-track, cross-track, and radial direction using BRDC as initial orbit is generally consistent with that using UR product. However, the orbit accuracy is lower at the beginning of the filter and the convergence time is longer than that of using the UR product. Besides, the optimal a priori STD magnitude using the BRDC product are about two orders of magnitude larger than that of the UR products, which is in accordance with the orbit accuracy of these two products.

Similar to the previous findings, the orbit accuracy becomes worse if the a priori STD is too small (see blue line in Figures 7 and 8). Table 9 gives the optimal a priori STD magnitude of SRP and PV parameters, which use the data in Table 2 as the base value. Moreover, the Time series of the average orbit accuracy using the optimal a priori STD magnitude is plotted in Figure 9. Even when the BRDC was used as the initial value, it can be seen that the orbit accuracy can reach to meter-level immediately after the filter startup. Meanwhile, the radial direction of the orbit can converge immediately since the SRP parameters are estimated by fitting the 3-day orbit arc, which results in the relatively high accuracy. Moreover, the optimal a priori STD magnitude of PV parameters of the broadcast ephemerides can be used as a reference after the orbit maneuver in next section.

**Table 8.** The average convergence time of the filter orbit using different a priori STD when the BRDC product is used as the initial orbit. Unit [hour]. For the GEO satellites, the convergence criteria adopted in our study are 100 cm in the along-track, and 80 cm in the cross-track and radial direction. For the IGSO and MEO satellites, the criteria are 60 cm in three directions.

$\sigma(\tilde{\epsilon}_0)$	GEO			IGSO			MEO		
	A	C	R	A	C	R	A	C	R
$10 \times \sigma_0(X_{srp})$	21.31	5.31	6.11	9.31	6.13	6.07	5.84	2.01	2.72
$100 \times \sigma_0(X_{srp})$	20.89	5.10	6.20	8.39	6.79	6.72	5.99	3.22	5.01
$1000 \times \sigma_0(X_{srp})$	20.47	5.24	12.64	11.06	8.52	16.56	6.14	4.98	9.39
$10 \times \sigma_0(X_{pv})$	30.86	6.21	17.40	15.16	13.57	18.45	9.03	6.72	10.84
$100 \times \sigma_0(X_{pv})$	20.81	10.13	15.66	10.23	7.48	18.23	6.40	4.51	9.93
$1000 \times \sigma_0(X_{pv})$	21.14	12.30	16.14	14.37	9.50	19.30	7.46	5.73	10.75
ref	20.74	12.33	16.12	14.59	10.08	19.52	7.39	5.93	10.82

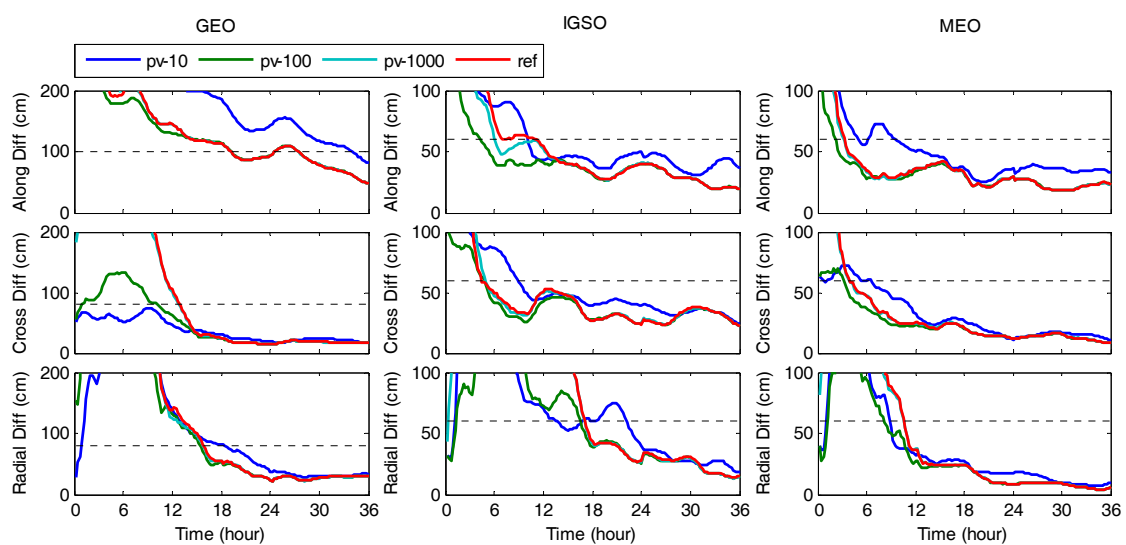


**Figure 7.** Time series of the average orbit accuracy using different a priori STD of PV parameters. The BRDC product is used as the initial orbit. The horizontal black dotted line represents the convergence criteria for each direction.

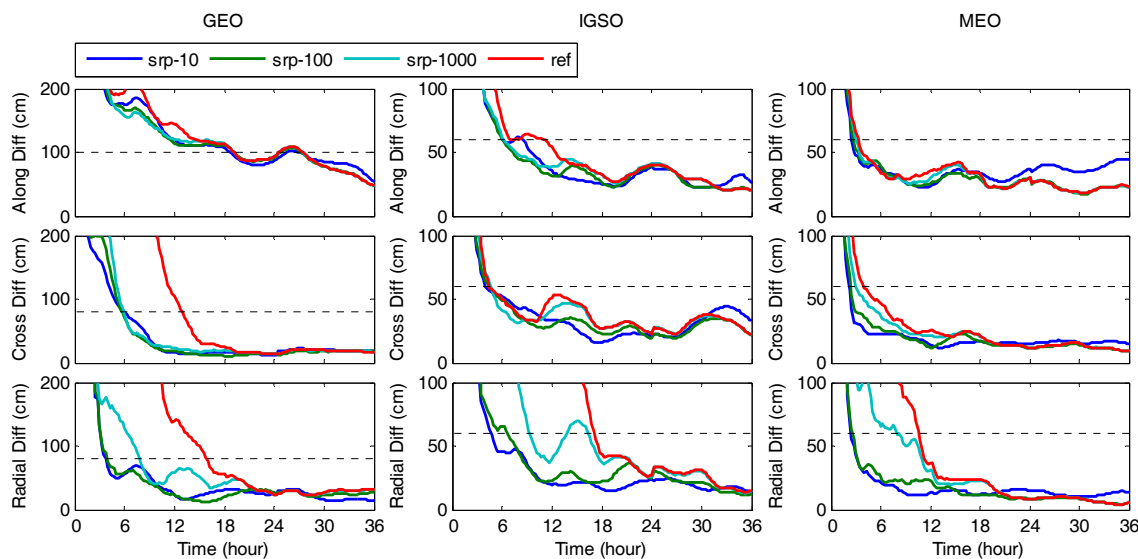


**Figure 8.** Time series of the average orbit accuracy using different a priori STD of SRP parameters. The BRDC product is used as the initial orbit. The horizontal black dotted line represents the convergence criteria for each direction.

**Table 9.** The optimal a priori STD magnitude of SRP and PV parameters when the BRDC product is used as the initial orbit.

Parameter	GEO	IGSO	MEO
SRP	$100 \times \sigma_0(X_{srp})$	$100 \times \sigma_0(X_{srp})$	$100 \times \sigma_0(X_{srp})$
PV	$100 \times \sigma_0(X_{pv})$	$100 \times \sigma_0(X_{pv})$	$100 \times \sigma_0(X_{pv})$

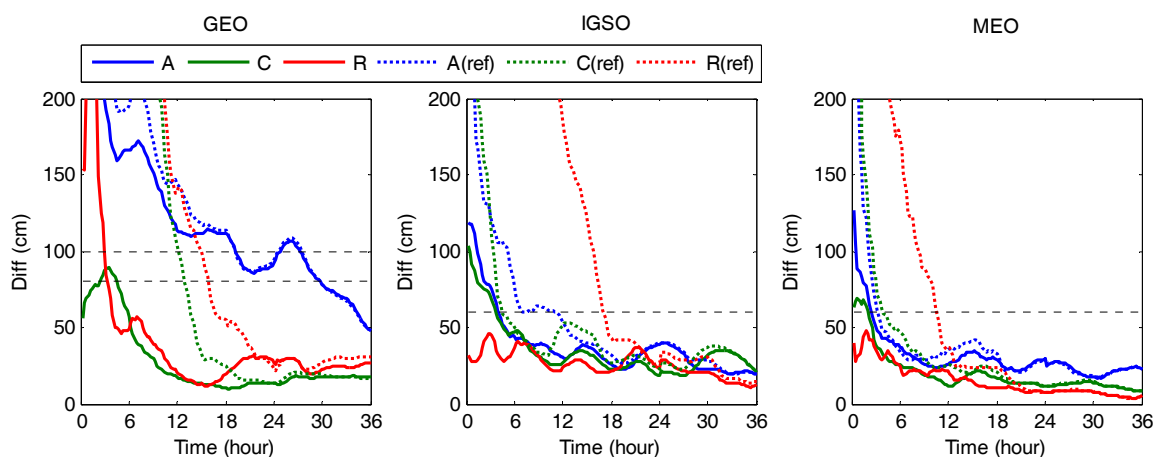


**Figure 9.** Time series of the average accuracy of the filter orbits with the optimal a priori STD magnitude. The BRDC product is used as the initial orbit. The dotted line represents the accuracy of the REF orbits described in Section 3.1. The horizontal black dotted line represents the convergence criteria for each direction.

### 3.4. Orbit Convergence after Maneuver

Orbit maneuver was analyzed as an example of orbit anomalies in this section. When the orbit maneuver occurs, the original orbit will be no longer accurate due to the external forces. The satellite orbit will deviate from the prediction orbit using the original dynamic model. For more intuitive illustration, Figure 10 illustrates a schematic diagram of the orbit change before and after the orbit

maneuver. After the orbit maneuver, usually the high-precision UR products cannot be obtained within 24 h while the broadcast ephemeris with lower precision can be accessible within a few hours.

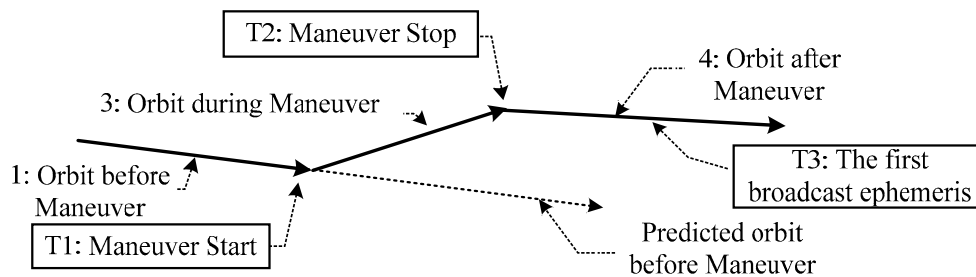


Figure 10. The orbit change before and after the orbit maneuver.

During the maneuver period, in order to accurately describe force models and keep the orbit accuracy high, additional forces should be estimated and process noise should be adjusted. In this paper, for simplicity, when the orbit maneuver is detected, the orbit estimation of the maneuvering satellite is stopped until the broadcast ephemeris can be received, which implies that the orbit maneuver is over. The second sets of experimental data described in Section 2.3 are used in this section. The PV parameters are initialized with the broadcast ephemerides. By comparison with the WHU final products, the broadcasted orbit accuracy of C05 is 6.4 m, 0.7 m and 1.0 m in the along-track, cross-track and radial directions respectively, and that of C08 is 4.0 m, 5.3 m and 3.1 m respectively. It can be seen that the accuracy of the broadcast ephemeris is worse than the normal case, which is because that the first group broadcast ephemeris after the orbit maneuver is estimated using short-arc. Concerning the deteriorating accuracy of the broadcast ephemeris after maneuver, combined with the analysis of Section 3.3, the looser a priori STD is set to  $\sigma(X_{pos}) = 100\text{ m}$ ,  $\sigma(X_{vel}) = 0.01\text{ m/s}$ , which is about one order of magnitude larger than the value in Table 9 to be in line with the orbit accuracy of the general situation after maneuver. As for the SRP parameters, it can be initialized with the estimated value by the filter before the orbit maneuver started and the a priori STD can be determined based on the a posteriori STD (Table 10) corresponding to this value. In addition, Table 10 shows that the a posteriori STD obtained from the filter has the same magnitude with the batch processing (Table 2). Considering that the satellite orbit changes before and after the orbit maneuver, the solar radiation pressure might fluctuate slightly. Therefore, different a priori STD (Table 11) of SRP parameters based on Table 10 was tested.

Table 10. A posteriori STD of the SRP parameters of the filter before the orbit maneuver.

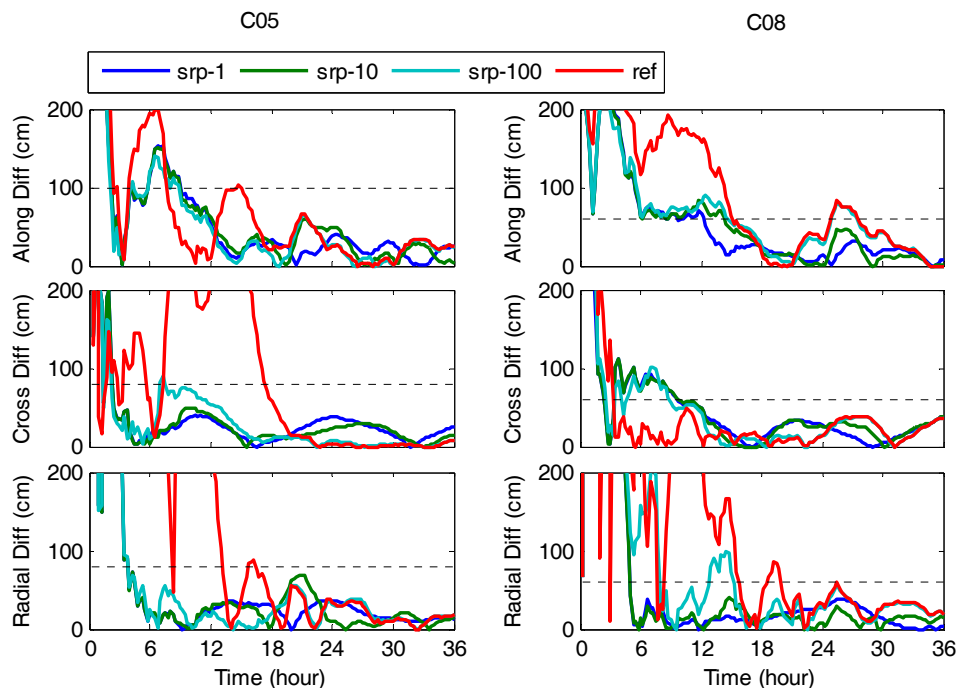
Type	$\sigma_0^m(X_{srp})$ (Unit: $\text{m/s}^2$ )				
	D0	Y0	B0	BC1	BS1
C05	$6.1 \times 10^{-12}$	$3.6 \times 10^{-12}$	$3.5 \times 10^{-11}$	$1.8 \times 10^{-10}$	$1.5 \times 10^{-10}$
C08	$2.2 \times 10^{-11}$	$5.8 \times 10^{-12}$	$6.0 \times 10^{-11}$	$1.5 \times 10^{-10}$	$6.8 \times 10^{-10}$

Table 11. The experiment scheme of the convergence analysis after the orbit maneuver.

Type	The A Priori STD		
SRP	$\sigma_0^m(X_{srp})$	$10 \times \sigma_0^m(X_{srp})$	$100 \times \sigma_0^m(X_{srp})$

From Section 2.3, it can be seen that the maneuver of C05 ends at 01:14 on DOY 187 and receive the first group of broadcast ephemeris at 06:00, and the maneuver of C08 ends at 14:50 on DOY 009 and receive the first group of broadcast ephemeris at 20:00. In this paper, the filter process of the maneuver satellite is restarted at the moment when the broadcast ephemeris is received and last for 36 h to study

the convergence performance after the orbit maneuver. Since the GBM product is unavailable in a short time after the maneuver, the orbits computed by the filter are evaluated by comparison with the WHU product. Figure 11 plots the time series of the orbit accuracy using different a priori STD (Table 11) of SRP parameters. For comparison, the accuracy of the orbit with loose a priori constraints (REF)  $X_{srp} = 0$ ,  $\sigma(X_{srp}) = 10^{-4} \text{ m/s}^2$  and  $\sigma(X_{pos}) = 100 \text{ m}$ ,  $\sigma(X_{vel}) = 0.01 \text{ m/s}$  are also given in red line.



**Figure 11.** Time series of the orbit accuracy using different a priori STD of SRP parameters. The horizontal black dotted line represents the convergence criteria for each direction.

Although the satellite orbit has changed by external forces, results show that the SPR parameters obtained before the maneuver is still effective as the initial value for convergence. The reason is that the solar radiation pressure is closely related to the satellite attitude, panel optical properties and distance between the satellite and the sun. After the end of the external forces, the satellite attitude will automatically adjust to normal attitude, the optical properties barely change, and the distance change from the satellite to the sun caused by the external forces is nearly negligible compared to its original distance. Therefore, the SPR parameters obtained before the maneuver occurs still work for the filter on the orbit determination. However, it can be observed that the orbits with tight constraints are relatively poor than the REF solution in the middle stage of the filter in terms of the accuracy in the along-track and cross-track of C05 and the cross-track of C08. Despite of this, the accuracy is acceptable and achieves the same accuracy eventually. Moreover, significant improvements can be found in the radial direction which affect the positioning accuracy the most, and the accuracy can reach less than 1 m within 6 h in the along-track, cross-track and radial direction.

For comparison, the accuracy of the broadcast ephemeris after maneuver is plotted in Figure 12, which is also compared with WHU product. It should be noted that the UR products are not available within one day after the maneuver, therefore, the only real-time orbit products users can obtain are the broadcast ephemeris. Figure 12 indicates that accuracy of the broadcast ephemerides provided to users after the maneuver is about 10 m or even worse. As shown in Figure 11, the real-time orbit accuracy within 1 m can be achieved in about 6 h after the filter startup, which illustrates the effectiveness of the proposed method. Therefore, it is of great significance using the SRP parameters obtained before the maneuver as the initial value with proper a priori STD constraints.

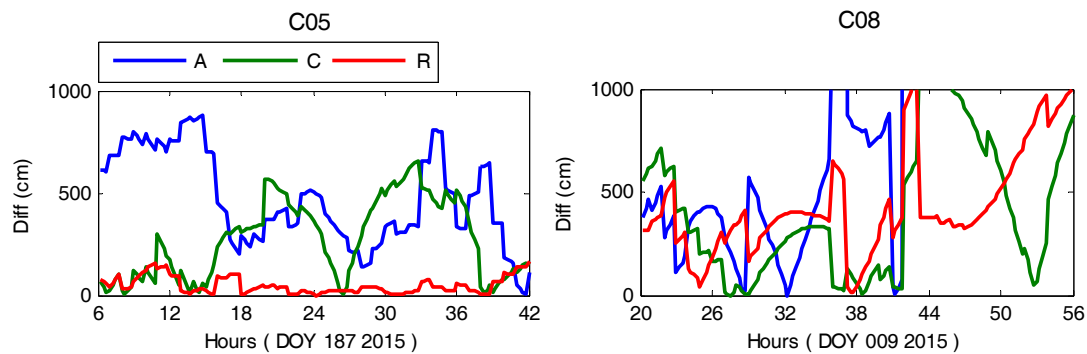


**Figure 12.** Accuracy of the broadcast ephemeris after the orbit maneuver. WHU product is used to evaluate the orbit accuracy.

#### 4. Discussion

Through the above analysis, we can see that using the UR and BRDC products as the initial orbit with appropriate a priori STD is of great significance on the orbit convergence performance. From the results of Sections 3.2 and 3.3, it can be seen that the convergence performance is acceptable with the a priori STD range from the optimal a priori STD magnitude (Tables 7 and 9) to 10 times the value. Therefore, in combination with the a posteriori STD of Table 3 as well as the optimal a priori STD magnitude of Tables 7 and 9, the appropriate range of a priori STD when using UR and BRDC products as the initial orbits are summarized in Table 12. These results can be used as references when the orbit filter starts up or restarts. Moreover, for the period after the maneuver, the real-time orbit accuracy can reach within 1 m in about 6 h after the first group of broadcast ephemeris is received. In summary, the accurate PV and SRP parameters with proper a priori STD can accelerate the filter convergence, and more importantly, it can provide more reliable orbit products after the orbit maneuver. In the future work, we could introduce additional forces and adjust process noise to generate the usable orbit products during the maneuver period. In this way, usable orbits could be obtained immediately at the end of maneuvers. Moreover, together with the SRP parameters estimated before the orbit maneuver and proper a priori STD constraints, high-precision orbit could be obtained more rapidly. This will be analyzed in the future study.

**Table 12.** The reference magnitude of a priori STD.

Initial Orbit Type	Satellite Type	PV (Unit: m; m/s)			SRP (Unit: m/s <sup>2</sup> )				
		Pos.	Vel.	D0	Y0	B0	BC1	BS1	
Ultra-Rapid Products	GEO	1~5	$(1\sim5) \times 10^{-4}$	$7 \times 10^{-11}$	$2 \times 10^{-11}$	$3 \times 10^{-10}$	$3 \times 10^{-9}$	$9 \times 10^{-10}$	
	IGSO	0.1~0.2	$(1\sim2) \times 10^{-5}$	$7 \times 10^{-12}$	$2 \times 10^{-12}$	$2 \times 10^{-11}$	$5 \times 10^{-11}$	$3 \times 10^{-11}$	
	MEO	0.1~0.2	$(1\sim2) \times 10^{-5}$	$4 \times 10^{-11}$	$2 \times 10^{-12}$	$3 \times 10^{-11}$	$2 \times 10^{-10}$	$6 \times 10^{-11}$	
Broadcast Ephemerides	GEO	10~50	$(1\sim5) \times 10^{-3}$	$7 \times 10^{-10}$	$2 \times 10^{-10}$	$3 \times 10^{-9}$	$3 \times 10^{-8}$	$9 \times 10^{-9}$	
	IGSO	1~2	$(1\sim2) \times 10^{-4}$	$7 \times 10^{-10}$	$2 \times 10^{-10}$	$2 \times 10^{-9}$	$5 \times 10^{-9}$	$3 \times 10^{-9}$	
	MEO	1~2	$(1\sim2) \times 10^{-4}$	$4 \times 10^{-09}$	$2 \times 10^{-10}$	$3 \times 10^{-9}$	$2 \times 10^{-8}$	$6 \times 10^{-9}$	

#### 5. Conclusions

Due to the limitations of the batch estimation processing real-time orbit method discussed earlier, such as orbit maneuver, the filter method was used to generate the real-time orbit in this paper. This paper mainly focuses on the influences of the initial values of the PV and SRP parameters on the convergence of filter in normal and abnormal (orbit maneuver) period.

For the normal period, the UR and BRDC products used as the initial orbits are discussed. In these two cases, the influences of the initial state (PV and SRP) are analyzed separately to obtain the optimal a priori STD magnitude. Results show that both PV and SRP parameters have positive effects on the orbit accuracy in the along-track, cross-track and radial directions for the GEO/IGSO/MEO satellites.

Besides, the high accuracy of the radial direction mainly relies on the accuracy of the SRP parameters, which is due to the highest accuracy of the dynamics model in the radial direction. Finally, the PV and SRP parameters with optimal a priori STD magnitude are both applied to the filter. The reference filter orbit using the loose a priori STD is also given for comparison. When the UR product is used as the initial orbit with optimal a priori STD magnitude, the orbit accuracy of the IGSO and MEO satellites can converge to decimeter-level immediately. However, the effect is less significant for the GEO satellites but still can reach to the meter-level accuracy rapidly. Similarly, when the BRDC is used as the initial orbit, the effect is not as obvious as that of the UR product, while much better than the reference solution. For the IGSO and MEO satellites, the meter-level orbit accuracy can be obtained immediately and reach to decimeter-level in about 6 h. As for the GEO satellites, meter-level accuracy can be obtained in about 3 h.

Orbit maneuver is taken as an example of orbit anomalies. When the orbit maneuver occurs, the batch estimation processing real-time orbits (the Ultra-Rapid products) are unavailable within 1 day. Therefore, it is meaningful to study how to speed up the convergence of the filter, so that the user can get more accurate orbits in shorter time. By using the SRP parameters estimated by the filter before the orbit maneuver as the initial value, along with proper a priori STD, the meter-level accuracy can be achieved in about 6 h after the first group of broadcast ephemerides are received, which is much higher than that of the broadcast ephemerides.

**Acknowledgments:** We thank the efforts of the IGS MGEX campaign in providing the multi-GNSS data. This work is supported by the National Key Research and Development Program of China (No. 2016YFB0501802). This work is supported by the China Postdoctoral Science Foundation Grant (No. 2017M612506).

**Author Contributions:** Yun Qing, Yidong Lou, Xiaolei Dai conceived and designed the experiments; Yun Qing performed the experiments, analyzed the data and wrote the first draft; Yidong Lou, Yang Liu and Yi Cai reviewed and revised the manuscript.

**Conflicts of Interest:** The authors declare no conflict of interest.

## References

1. BeiDou Satellite Navigation System. Available online: <http://www.beidou.gov.cn/> (accessed on 4 November 2017).
2. Tapley, B.; Schutz, B.; Born, G.H. *Statistical Orbit Determination*; Elsevier Academic Press: Cambridge, MA, USA, 2004.
3. Ge, M.; Zhang, H.P.; Jia, X.L.; Song, S.L.; Wickert, J. What is achievable with the current compass constellation. *GPS World* **2012**, *1*, 29–34.
4. Shi, C.; Zhao, Q.; Li, M.; Tang, W.; Hu, Z.; Lou, Y.; Zhang, H.; Niu, X.; Liu, J. Precise orbit determination of BeiDou satellites with precise positioning. *Sci. China Earth Sci.* **2012**, *55*, 1079–1086. [[CrossRef](#)]
5. Montenbruck, O.; Hauschild, A.; Steigenberger, P.; Hugentobler, U.; Teunissen, P.; Nakamura, S. Initial assessment of the COMPASS/BeiDou-2 regional navigation satellite system. *GPS Solut.* **2013**, *17*, 211–222. [[CrossRef](#)]
6. Zhao, Q.; Guo, J.; Li, M.; Qu, L.; Hu, Z.; Shi, C.; Liu, J. Initial results of precise orbit and clock determination for COMPASS navigation satellite system. *J. Geodesy* **2013**, *87*, 475–486. [[CrossRef](#)]
7. Steigenberger, P.; Hugentobler, U.; Hauschild, A.; Montenbruck, O. Orbit and clock analysis of Compass GEO and IGSO satellites. *J. Geodesy* **2013**, *87*, 515–525. [[CrossRef](#)]
8. Zhou, S.; Hu, X.; Zhou, J.; Chen, J.; Gong, X.; Tang, C.; Wu, B.; Liu, L.; Guo, R.; He, F.; et al. Accuracy Analyses of Precise Orbit Determination and Timing for COMPASS/BeiDou-2 4GEO/5IGSO/4MEO Constellation. In Proceedings of the China Satellite Navigation Conference (CSNC), Wuhan, Hubei, China, 15–17 May 2013; pp. 89–102.
9. Liu, Y.; Lou, Y.; Shi, C.; Zheng, F.; Yin, Q. BeiDou Regional Navigation System Network Solution and Precision Analysis. In Proceedings of the China Satellite Navigation Conference (CSNC), Wuhan, Hubei, China, 15–17 May 2013; pp. 173–186.
10. He, L.; Ge, M.; Wang, J.; Wickert, J.; Schuh, H. Experimental study on the precise orbit determination of the BeiDou navigation satellite system. *Sensors* **2013**, *13*, 2911–2928. [[CrossRef](#)] [[PubMed](#)]

11. Deng, Z.; Fritsche, M.; Uhlmann, M.; Wickert, J.; Schuh, H. Reprocessing of GFZ multi-GNSS Product GBM. In Proceedings of the IGS Workshop, Sydney, Australia, 8–12 February 2016; pp. 8–12.
12. Liu, J.; Gu, D.; Ju, B.; Shen, Z.; Lai, Y.; Yi, D. A new empirical solar radiation pressure model for BeiDou GEO satellites. *Adv. Space Res.* **2016**, *57*, 234–244. [[CrossRef](#)]
13. Tan, B.; Yuan, Y.; Zhang, B.; Hsu, H.Z.; Ou, J. A new analytical solar radiation pressure model for current BeiDou satellites: IGGSPM. *Sci. Rep.* **2016**, *6*, 32967. [[CrossRef](#)] [[PubMed](#)]
14. Guo, J.; Chen, G.; Zhao, Q.; Liu, J.; Liu, X. Comparison of solar radiation pressure models for BDS IGSO and MEO satellites with emphasis on improving orbit quality. *GPS Solut.* **2017**, *21*, 511–522. [[CrossRef](#)]
15. Montenbruck, O.; Steigenberger, P.; Prange, L.; Deng, Z.; Zhao, Q.; Perosanz, F.; Romero, I.; Noll, C.; Stürze, A.; Weber, G.; et al. The Multi-GNSS Experiment (MGEX) of the International GNSS Service (IGS)—Achievements, prospects and challenges. *Adv. Space Res.* **2017**, *59*, 1671–1697. [[CrossRef](#)]
16. Prange, L.; Orliac, E.; Dach, R.; Arnold, D.; Beutler, G.; Schaer, S.; Jäggi, A. CODE’s five-system orbit and clock solution—The challenges of multi-GNSS data analysis. *J. Geodesy* **2017**, *91*, 345–360. [[CrossRef](#)]
17. Guo, J.; Zhao, Q.; Geng, T.; Su, X.; Liu, J. Precise Orbit Determination for COMPASS IGSO Satellites During Yaw Maneuvers. In Proceedings of the China Satellite Navigation Conference (CSNC), Wuhan, Hubei, China, 15–17 May 2013; pp. 41–53.
18. Dai, X.; Ge, M.; Lou, Y.; Shi, C.; Wickert, J.; Schuh, H. Estimating the yaw-attitude of BDS IGSO and MEO satellites. *J. Geodesy* **2015**, *89*, 1005–1018. [[CrossRef](#)]
19. Lou, Y.; Liu, Y.; Shi, C.; Wang, B.; Yao, X.; Zheng, F. Precise orbit determination of BeiDou constellation: Method comparison. *GPS Solut.* **2016**, *20*, 259–268. [[CrossRef](#)]
20. Bertiger, W.I.; Bar-Sever, Y.E.; Haines, B.J.; Iijima, B.A.; Lichten, S.M.; Lindqwister, U.J.; Romans, L.J. A Real-Time Wide Area Differential GPS System. *Navigation* **1997**, *44*, 433–447. [[CrossRef](#)]
21. Bertiger, W.; Bar-Sever, Y.; Bokor, E.; Butala, M.; Dorsey, A.; Gross, J.; Harvey, N.; Lu, W.; Miller, K.; Miller, M.; et al. First Orbit Determination Performance Assessment for the OCX Navigation Software in an Operational Environment. In Proceedings of the 25th International Technical Meeting of the Satellite Division of the Institute of Navigation (ION GNSS+ 2012), Nashville, TN, USA, 17–21 September 2012.
22. Leandro, R.; Landar, H.; Nitschke, M.; Glocker, M.; Seeger, S.; Chen, X.; Deking, A.; BenTahar, M.; Zhang, F.; Ferguson, K.; et al. RTX Positioning: The Next Generation of Cm-Accurate Real-time GNSS Positioning. In Proceedings of the 24th International Technical Meeting of The Satellite Division of the Institute of Navigation (ION GNSS 2011), Portland, OR, USA, 20–23 September 2011.
23. Glocker, M.; Landau, H.; Leandro, R.; Nitschke, M. Global Precise Multi-GNSS Positioning with Trimble Centerpoint RTX. In Proceedings of the Satellite Navigation Technologies and European Workshop on GNSS Signals and Signal Processing, (NAVITEC), Noordwijk, The Netherlands, 5–7 December 2012; pp. 1–8.
24. Kazmierski, K.; Sośnica, K.; Hadas, T. Quality assessment of multi-GNSS orbits and clocks for real-time precise point positioning. *GPS Solut.* **2018**, *22*, 11. [[CrossRef](#)]
25. Dow, J.; Martin Mur, T.; Feltens, J.; Martinez, C.G. The ESOC GPS Facility: Report on the IGS 1992 Campaign and Outlook. In Proceedings of the IGS Workshop, Bern, Switzerland, 25–26 March 1993; pp. 133–144.
26. Dow, J.M.; García, C.; Feltens, J.; Springer, T.; Perez, J.; Boomkamp, H.; Rojo, E.; Romero, I. *The ESA/ESOC IGS Analysis Centre Annual Report 2003–2004*; ESA/European Space Operations Centre: Darmstadt, Germany, 2005.
27. Zhang, Q.; Moore, P.; Hanley, J.; Martin, S. Auto-BAHN: Software for near real-time GPS orbit and clock computations. *Adv. Space Res.* **2007**, *39*, 1531–1538. [[CrossRef](#)]
28. Liu, J.; Ge, M. PANDA software and its preliminary result of positioning and orbit determination. *Wuhan Univ. J. Nat. Sci.* **2003**, *8*, 603–609.
29. Lou, Y.; Liu, Y.; Shi, C.; Yao, X.; Zheng, F. Precise orbit determination of BeiDou constellation based on BETS and MGEX network. *Sci. Rep.* **2014**, *4*. [[CrossRef](#)] [[PubMed](#)]
30. Dilssner, F.; Springer, T.; Schönemann, E.; Enderle, W. Estimation of satellite antenna phase center corrections for BeiDou. In Proceedings of the IGS Workshop, Pasadena, CA, USA, 23–27 June 2014.
31. Springer, T.A.; Beutler, G.; Rothacher, M. A new solar radiation pressure model for GPS satellites. *GPS Solut.* **1999**, *2*, 50–62. [[CrossRef](#)]
32. Springer, T.A.; Beutler, G.; Rothacher, M. Improving the orbit estimates of GPS satellites. *J. Geodesy* **1999**, *73*, 147–157. [[CrossRef](#)]

33. Arnold, D.; Meindl, M.; Beutler, G.; Dach, R.; Schaer, S.; Lutz, S.; Prange, L.; Sośnica, K.; Mervart, L.; Jäggi, A.; et al. CODE's new solar radiation pressure model for GNSS orbit determination. *J. Geodesy* **2015**, *89*, 775–791. [[CrossRef](#)]
34. Petit, G.; Luzum, B. *IERS Conventions 2010. No. 36 in IERS Technical Note*; Verlag des Bundesamts für Kartographie und Geodäsie: Frankfurt am Main, Germany, 2010.
35. Rebischung, P.; Griffiths, J.; Ray, J.; Schmid, R.; Collilieux, X.; Garayt, B. IGS08: The IGS realization of ITRF2008. *GPS Solut.* **2012**, *16*, 483–494. [[CrossRef](#)]
36. Bizouard, C.; Gambis, D. The Combined Solution C04 for Earth Orientation Parameters Consistent with International Terrestrial Reference Frame 2008. In *Geodetic Reference Frames*; Springer: Berlin/Heidelberg, Germany. Available online: <http://citeseerx.ist.psu.edu/viewdoc/download?doi=10.1.1.734.6186&rep=rep1&type=pdf> (accessed on 15 January 2018).
37. Bierman, G.J. *Factorization Methods for Discrete Sequential Estimation*; Academic Press Inc.: New York, NY, USA, 1977.
38. Wessel, P.; Smith, W.H. New, improved version of Generic Mapping Tools released. *Eos* **1998**, *79*, 579. [[CrossRef](#)]



© 2018 by the authors. Licensee MDPI, Basel, Switzerland. This article is an open access article distributed under the terms and conditions of the Creative Commons Attribution (CC BY) license (<http://creativecommons.org/licenses/by/4.0/>).